Carbohydrate Polymers 84 (2011) 872–880

Contents lists available at ScienceDirect

Carbohydrate Polymers

journal homepage: www.elsevier.com/locate/carbpol

Stoichiometric interpretation of thermoplastic starch water sorption and relation to mechanical behavior

Farouk Ayadi*, Patrice Dole

Equipe Transformations Physico-chimiques des Matériaux Lignocellulosiques, UMR FARE, INRA, Campus Moulin de la Housse, Bâtiment 18 – 51687 Reims Cedex 2, France

ARTICLE INFO

Article history:
Received 10 September 2010
Received in revised form
29 November 2010
Accepted 8 December 2010
Available online 15 December 2010

Keywords:
Plasticized starch
Glycerol
Interaction stoichiometry
Cellulose

ABSTRACT

The characterization of glycerol plasticized starch by water sorption was interpreted in terms of interaction stoichiometry. The saturation of starch was found to correspond to a 2:1 anhydroglucose unit/glycerol stoichiometric ratio. The introduction of cellulose into the formulation of plasticized starch (TPS) decreased the quantity of bonded glycerol, due to the strong interaction between cellulose and starch. The systematic study of the TPS properties in the whole range of relative humidities showed transitions which were not connected to the "saturation transition" or to the glass transition. Breaking properties probably depended on a complex combination of different system characteristics.

1. Introduction

For several decades, starch, an abundant natural resource, has been considered to be a potential substitute for the polymer matrix in the formulation of thermoplastic materials (Anglès & Dufresne, 2001; Averous & Fringant, 2001; Averous, Moro, Dole, & Fringant, 2000; Baumberger, Lapierre, Monties, Lourdin, & Colonna, 1997; Baumberger, Lapierre, Monties, & Valle, 1998; Chang, Cheah, & Seow, 2000; Curvelo, de Carvalho, & Agnelli, 2001; de Carvalho, Curvelo, & Agnelli, 2001; Forssell, Hulleman, Myllärinen, Moates, & Parker, 1999; Hulleman, Janssen, & Feil, 1998; Lourdin, Valle, & Colonna, 1995; Lourdin, Bizot, & Colonna, 1997; Lourdin, Colonna, Brownsey, Noel, & Ring, 2002; Martin & Avérous, 2001; Myllärinen, Partanen, Seppälä, & Forssell, 2002; Rindlav-Westling, Stading, Hermansson, & Gatenholm, 1998; Shogren & Jasberg, 1994; Van Soest & Borger, 1997). Despite numerous advantages compared to synthetic polymers, most commercial materials use starch as a minor component in formulation, such as a filler or a dispersed polymer in a synthetic polymer matrix. The only commercial systems which use starch as a major component also add hydroxylated macromolecules (polyvinyl alcohol or cellulosic micro and nanofillers) to increase starch intrinsic strength. Follain, Joly, Dole, and Bliard (2005) have compared the numerous modifications of thermoplastic starch proposed in the literature and came to the conclusion that the best mechanical strategies depended on the plasticizer level used in the formulation. The mechanical behavior of highly plasticized material is affected by phase separation phenomena. Material improvement could be achieved, for example, by using plasticizer blends which limit the appearance of enriched phases. Materials formulated with medium plasticizer content (typically 20–25% for the starch/glycerol system) are mainly affected by starch intrinsic properties: amylopectin, the major component of starch is too highly branched to establish favorable entanglements between macromolecules (Monnet, Joly, Dole, & Bliard, 2010). Moreover, its recrystallization during aging (retrogradation) does not favor the opening of branched structures, which is necessary for the establishment of intermolecular interactions and entanglements. The improvement of medium plasticized starch would involve a modification of the chemical structure of amylopectin. The last type of polymer material, with low plasticizer content, is generally at the glassy state at room temperature. These materials exhibit low elongations at break and high strengths. These mechanical characteristics are obviously associated with the glassy state, but also with the high capacity of poorly plasticized starch to established strong H-bond interactions between macromolecules.

Godbillot, Dole, Joly, Rogé, and Mathlouthi (2006) used water as a chemical probe for the study of starch glycerol interactions. The equilibrium water content of glycerol plasticized starch does not vary continuously as a function of glycerol content: strongly bonded glycerol decreases the number of water sorption sites, and thus contributes to a decrease in water sorption. On the contrary,

---

* Corresponding author. Tel.: +33 326918490.
E-mail addresses: Farouk.ayadi@reims.inra.fr (F. Ayadi), Patrice.dole@reims.inra.fr (P. Dole).

0144-8617/$ – see front matter © 2010 Elsevier Ltd. All rights reserved.
doi:10.1016/j.carbpol.2010.12.024

excess glycerol increases water sorption, due to its high intrinsic hydrophilicity (Cho & Rhee, 2002).

Starch saturation by glycerol is a function of water activity. By extrapolating to zero water content, Godbillot et al. (2006) showed that the maximum glycerol content bonded onto starch was 23%. The authors proposed a chemical interpretation of this value, corresponding to 1:2 ratio of glycerol to anhydroglucose units.

The same method for starch material water sorption isotherms was used by Yu, Wang, Wu, and Zhu (2008) to study montmorillonite filled oxidized starch materials. In this work, a saturation point of 15% was found. This drastic difference compared to previous work can be attributed either to the type of starch used (origin, chemical oxidation modification), or to the effect of the filler system, selected in order to exhibit strong interactions with the matrix (Chivrac, Pollet, Schmutz, & Avérous, 2008).

Several studies demonstrated the general interest in cellulose fibers used as reinforcement for thermoplastic starch (Avérous, Fringant, & Moro, 2001; Curvelo et al., 2001; Ma, Yu, & Kennedy, 2005; Müller, Laurindo, & Yamashita, 2009). Indeed, both starch and cellulose are polymers of glucose. In cellulose, the glucose units are linked by 1–4 beta-likages, while in starch, the glucose units are linked by 1–4 alpha-likages.

In this paper, we wish to reevaluate the results of Godbillot et al. (2006), with more precise water sorption analysis using a dedicated sorption balance. Compared to the previous study, our work is based on corn starch. A further objective is to study the evolution of the glycerol saturation point when interacting filler is added to the formulation. Indeed, the use of starch in biocomposites is a general trend in the literature dedicated to natural polymers (Zhao, Torley, & Halley, 2008). Both water sorption and mechanical properties will be studied, in order to establish the relationship between phase diagrams of starch/water/glycerol/cellulose systems and the macroscopic mechanical behavior.

Table 1
TPS/cellulose formulations and glycerol content.

TPS			Cellulose film	
% Glycerol content (HPLC measurement)	% Cellulose added	Denoted blends	% Glycerol content	Denoted films
0	0	S0G	0	C
	5	S0G5C		
	10	S0G10C		
	20	S0G20C		
5.85 ± 0.28	0	S6G	5	C5G
	5	S6G5C		
	10	S6G10C		
	20	S6G20C		
11.16 ± 0.3	0	S11G	10	C10G
	5	S11G5C		
	10	S11G10C		
	20	S11G20C		
15.42 ± 0.32	0	S15G	15	C15G
	5	S15G5C		
	10	S15G10C		
	20	S15G20C		
19.02 ± 0.27	0	S19G	20	C20G
	5	S19G5C		
	10	S19G10C		
	20	S19G20C		
23.84 ± 0.33	0	S24G	25	C25G
	5	S24G5C		
	10	S24G10C		
	20	S24G20C		
28.26 ± 0.84	0	S28G	30	C30G
	5	S28G5C		
	10	S28G10C		
	20	S28G20C		
31.98 ± 1.31	0	S32G	35	C35G
	5	S32G5C		
	10	S32G10C		
	20	S32G20C		

2. Material and methods

2.1. Materials

The starch used in this work was extracted from corn flour provided by Ceregrain (Bourg en Bresse, France). It contained approximately (80–85%) starch (about 23% amylose and 77% amylopectin), (8–12%) protein, (4–5%) lipid and (1–2%) of cellulose.

40 L of cyclohexan (Carlo Erba reactifs SA, purity 99%) were used to extract lipids from 5 kg of corn flour (the mixture was left to stand for 12 h and mixed for four hours). About 4.5 kg of degreased corn flour were added to 10 L of distilled water containing sodium hydrogen sulfite ($NaHSO_3$) to prevent bacterial growth. The mixture was maintained at 50 °C for about 18–20 h with intermittent circulation of the liquid. The mixture was then left to rest for half an hour and then sieved using a vibratory sifter (FRITCH, analysette 3 PRO) meshe 20 μm. The residue was washed with distilled water until completely free of starch. The starch–protein slurry was left for 4–5 h and afterwards centrifuged at 2800 rpm for 5 min using a centrifuge (PROLABO, X230 model). The upper non-white layer was scraped off. The white layer was resuspended in distilled water and recentrifuged 3–4 times before being collected. Then the white dough was dried in a ventilated oven at 40 °C for 12 h. Finally, the obtained starch was conditioned at 50% HR during two weeks.

2.1.1. Cellulose

Natural cellulose fiber from leafwood having a diameter of 20 μm and a length of 60 μm was supplied by JRS (Arbocel, Germany). Amash and Zugenmaier (2000) have presented some characteristics of this cellulose and have reported the density to be 1.5 and the cellulose content higher than 99.5%.

2.1.2. Sample preparation

2.1.2.1. Plasticization and blend preparation. Processing began with blend preparation. Corn starch (containing 12% of moisture) was weighted and introduced into a turbo-mixer. After addition of glycerol, the two compounds were mixed at high speed (2000 rpm). Glycerol had a 99% purity grade according to the supplier (Carlo Erba reactifs SA), and was used without further purification. In order to make extrusion easier for blends containing less than 25% glycerol, a certain quantity of water was added so as to have a plasticizer level (water + glycerol) of 25% minimum. Various thermoplastic starch (TPS) formulations with different plasticizer/starch ratios were tested to obtain a wide range (see Table 1).

2.1.3. Processing conditions

Blends were extruded on a single screw extruder (SCAMIA S 2032, France) equipped with a conical-shaped element (see description and figures in Onteniente, Etienne, Bureau, and Claude (1996)). This design was suitable to provide high shearing. The screw of diameter 32 mm with a length 640 mm had two heating zones situated around the head (115 °C) and at the die (95 °C), while the screw speed was set at 25 rpm. Specific mechanical energy was 526 J/g. Finally, the extruded blends were granulated (2 mm of diameter).

The different plastic granules obtained above were each reinforced by 5, 10 and 20% of cellulose. These mixtures were manually fed into the extruder. The obtained composites were granulated and then extruded again to improve the dispersion of cellulose in the matrix. The last two extrusions were made at 45 rpm in a three zone single-screw extruder (Scamex-France), heated to 120, 120, and 110 °C, respectively. The screw was 220 mm long and the L/D ratio was equal to 11.

2.2. Methods

2.2.1. Differential scanning calorimetry

2.2.1.1. Starch transformation levels. Differential scanning calorimetry was used to ensure that the obtained pellets were completely amorphous. DSC experiments were performed with a DSC 2920 (TA instruments, France). Sample (20 mg) and deionised water (100 mg) were weighed directly in the pan and sealed hermetically. Pans were heated from −10 to 140 °C at a rate of 5 °C min^{-1}.

2.2.2. Specimen preparation and mechanical tests

The pellets obtained by extrusion processing were transformed into tensile samples (ISO 527-2 5A), approximately 2.5 mm thick, using a DSM Xplore 12 ml injection molding machine with a compressed air plunger. The experimental molding conditions were: temperature profile: 140 °C; injection pressure: 15 bar, mold temperature: 25 °C.

The samples were hydrated for at least ten days in RH (relative humidity) chambers controlled by saturated salt solutions at 20 °C. A total of 5 saturated salt solutions, LiCl (∼13.5% RH), $MgCl_2$ (∼37% RH), NaBr (∼54% RH), $CuCl_2$ (∼69% RH) and KCl (∼83% RH), were used to maintain specified relative humidities in the closed chambers.

A tensile test machine (TEST 108 2 kN from GT-TEST company, France) equipped with a load cell of 2 kN was used for tensile measurements. Strength, modulus and elongation at break were measured with a crosshead speed of 1 mm min^{-1} under constant conditions (50% RH, 20 °C) in an environmentally controlled room. Five measurements were conducted for each sample, and the results were averaged to obtain a mean value.

The tensile strength was calculated from the initial sample section which was systematically measured before mechanical testing.

2.2.3. Film preparation and water sorption

TPS and cellulose/TPS extruded pellets were transformed into films, having an average thickness of approximately 100 μm, using a manual 15 ton press (from "Specac", UK) with heated plates. The temperature of the heated plates was 90 °C. The cellulose/glycerol films were prepared by a casting method (this system is not sufficient to obtain an extruded material), using 100 ml of distilled water containing 4% cellulose (weight). Glycerol was used as plasticizer, at concentrations from 0 to 0.35 g/g dry cellulose divided in 0.05 g increments. The solution was evenly spread on Teflon coated plates placed on an oil bath heated to 90 °C until adhesion between the film and the plate disappeared.

Sorption isotherms at 20 °C for starch, cellulose and starch/cellulose films with different glycerol contents were obtained using a dynamic vapor sorption system (IGA-sorption measurements, UK). This technique is based on an ultrasensitive balance capable of measuring changes in the sample mass as low as 0.01 mg. The sample is equilibrated at a constant temperature at different relative humidities. The changes in relative humidity were induced by mixtures of dry and moisture-saturated nitrogen flowing over the samples. The sample mass used was about 3–5 mg, and the programmed relative humidities were from 0 to 80%, divided in 10% increments (9 points). The temperature was set at 20 °C. The samples were considered to be at equilibrium when it reaches less than 2% of asymptotic's mass change (the IGA real time processor uses least-squares regression model in order to extrapolate the value of the asymptote).

The sample was dried to constant mass under a stream of dry nitrogen (0% RH) to obtain the dried weight.

2.2.4. Assay of glycerol by HPLC

The glycerol content in various thermoplastic starch (TPS) formulations was determined using a customized Waters HPLC system, equipped with a Waters 600 HPLC pump, a Waters 710plus automated injector, a Jasco CO-965 column oven, a Waters 410 Refractive Index detector and an Alltimer HP C18 AQ 5 mm column (250 mm × 4.6 mm). An isocratic mobile phase composed of water was used. Flow rate was 1 ml/min. The temperature of the column oven was set at 35 °C. All of the chromatographic data management was ensured by the Empower software 2.0 version (Waters). Analyses were performed on samples at approximately 1 g/L. Water was used for sample preparation, except for the water effect analysis for which the crude reaction mixtures were injected. An injection volume of 10 μl was eluted at 1 ml/min during an acquisition period of 8 min.

2.2.5. Investigation of SEM pictures

Scanning electron microscopy micrographs of Native cellulose was obtained with a scanning electron microscope; model MEB XL 30 from PHILIPS. The sample was fixed on carbon adhesive bearings and coated with gold–palladium using a plasma sputtering apparatus, model SCD 040 from BALZERS, prior to SEM investigation.

2.2.6. X-ray (RX)

Diffraction diagram of 1 g of cellulose was recorded using Brucker advance D8 (Montage of Bragg Brentano: mirror of göbel). X-ray equipment operating at 40 kV and 40 mA. Detector Scintillation counter was used to monitor the diffracted intensities. The diffractogram was normalized at the same total area under scattering curve over the Bragg angle range 3° and 30° (2θ).

3. Results and discussion

3.1. Glycerol content and starch transformation level

Table 1 shows the different TPS/cellulose formulations and the results of glycerol assays performed by HPLC (the results from the duplicate experiments were averaged).

Experiments performed by DSC from all samples show a flat thermogram (the gelatinization enthalpy value was 0), which proved that obtained pellets were amorphous after extrusion.

3.2. Water sorption

3.2.1. Characterization of reference materials

Fig. 1 shows the water sorption isotherms of the components used in this study. The filler system used was selected for its high interaction capacity, in order to enhance the effect of filler on the behavior of the starch glycerol system. A duplicate experiment of water sorption results were averaged and the standard deviation of each relative humidity (10, 20, 30, 40, 55, 70, 80% RH) was respectively (0.14, 0.23, 0.19, 0.33, 0.87, 1.39, 2.04% of water uptake). The commercially pure cellulose additive was obtained by a drastic milling which reduced the system granulometry (see SEM picture in Fig. 2a).

Fig. 2b shows the RX spectra of the cellulose sample, which shows only two broad peaks centered at $2\theta = 15.5$ and 22.5. The determination of the % of crystallinity of cellulose was based on peak heights (intensity) using the empirical relationship (Subramanian, Senthil Kumar, Jeyapal, & Venkatesh, 2005):

$$\%\ \text{Crystallinity} = \left(\frac{I_{002} - I_{18.5}}{I_{002}}\right) \times 100$$

where I_{002} is the Bragg peak height at $2\theta = 22.5°$ and $I_{18.5}$ is the height for the amorphous background at $2\theta = 18.5°$ (Fig. 2b). The intensity (peak height) of the diffracted X-ray beam from 0 0 2

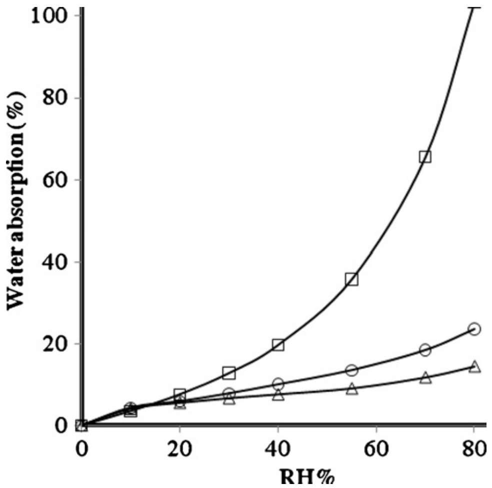

Fig. 1. Sorption isotherms for starch (○), glycerol (□) and cellulose (△).

($2\theta = 22.5^\circ$) plane of cellulose has been assigned to its crystalline region and the intensity of the scattered X-ray (at the minimum between the large Bragg peak and the immediate small Bragg peak at its left), at $2\theta = 18.5^\circ$ is attributed to the amorphous back ground of the cellulose. The % crystallinity of this cellulose is 66% (Helbert, Sugiyama, Ishihara, & Yamanaka, 1997; Ishikawa, Okano, & Sugiyama, 1997).

As a result, the water sorption isotherms of starch and cellulose (Fig. 1) show identical behavior at low RH, the amount of sorption sites of both polysaccharides being almost identical. For higher relative humidity, starch and cellulose show different behavior, as the residual cellulose organization limits the swelling of the system.

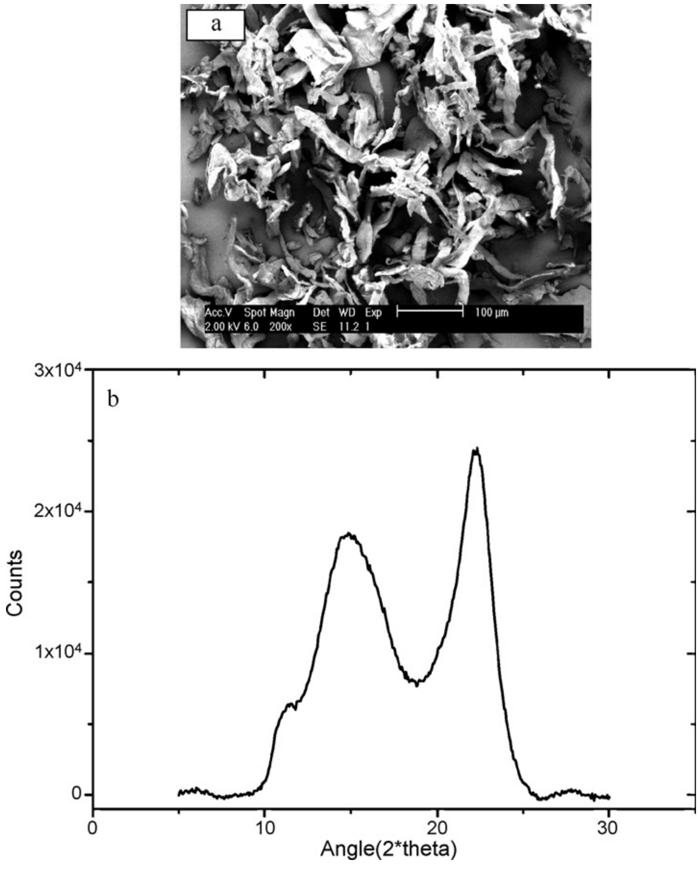

Fig. 2. (a) Scanning electron microscopy of cellulose and (b) diffractograms of cellulose conditioned at 50% RH.

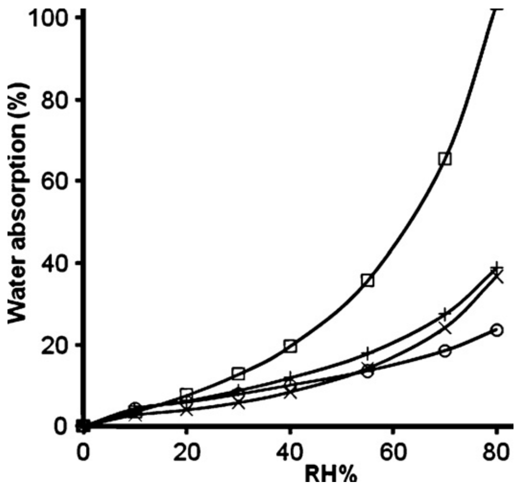

Fig. 3. Sorption isotherms for starch (○), glycerol (□), starch + 19% glycerol calculated (+) and starch + 19% glycerol experimental (×).

3.2.2. *Characterization of the starch glycerol system*

As shown in Fig. 1, glycerol represents the highest hydrophilicity. Theoretically, the addition of noninteracting glycerol molecules in a starch or cellulose system should lead to an increase in hydrophilicity.

Fig. 3 compares the experimental sorption behavior of a 19% glycerol plasticized starch to a calculated isotherm assuming a simple linear mixing law, obtained from the experimental behavior of pure components. At low relative humidity, the experimental sorption isotherm shows lower values than the calculated ones. This has been already presented by Lourdin, Coignard, Bizot, and Colonna (1997) and attributed to the strong interactions between starch and glycerol, which reduce the number of water sorption sites.

For high RH, the experimental values are closer to the theoretical isotherm, suggesting a higher amount of glycerol molecules showing intrinsic hydrophilic properties.

3.2.3. *Characterization of the cellulose glycerol system*

The cellulose glycerol system presents behavior similar to the plasticized starch. The experimental water sorption of the cellulose glycerol system (Fig. 4) shows lower hydrophilicity than that calculated from a mixing law of pure component behavior. Moreover, at low relative humidity, the quantity of sorbed water is even lower than that of both components individually. Again, the strong interactions of a part of the glycerol introduced in the formulation with the polysaccharide leads to a decrease in water content.

3.2.4. *Characterization of the cellulose glycerol starch system*

Fig. 5 compares the sorption isotherms of cellulose plasticized starch material to the reference isotherms of cellulose and corresponding plasticized starch. As previously observed, the complex system presents a lower hydrophilicity at low RH compared to the behavior of both components individually. This suggests a cumulative effect of glycerol interaction with starch and cellulose, and/or specific interactions of starch and cellulose.

3.2.5. *Calculated and experimental phase diagrams*

Water sorption isotherms of binary systems can be analyzed by plotting the water content as a function of the plasticizer content for each relative humidity. Fig. 6a and b shows the experimental diagrams obtained from starch–glycerol and cellulose–glycerol systems. A typical sheaf of curves is obtained which confirms pre-

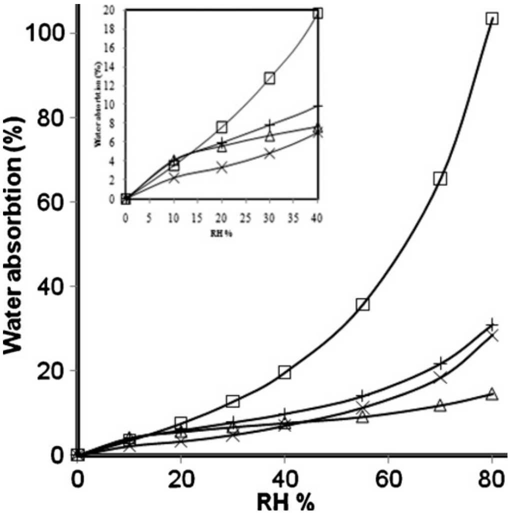

Fig. 4. Sorption isotherms for cellulose (△), glycerol (□), calculated cellulose +19% glycerol (+) and experimental cellulose +19% glycerol (×).

vious results (Godbillot et al., 2006): at low relative humidities and low glycerol content, water content decreased as a function of the plasticizer content, suggesting a direct competition of glycerol and water molecules for the sorption onto polysaccharides. The existence of a linear relationship suggests simple partition rules (Kristo & Biliaderis, 2006; Talja, Helén, Roos, & Jouppila, 2007).

For high glycerol content, the introduction of glycerol leads to a linear increase in hydrophilicity, suggesting that in this area

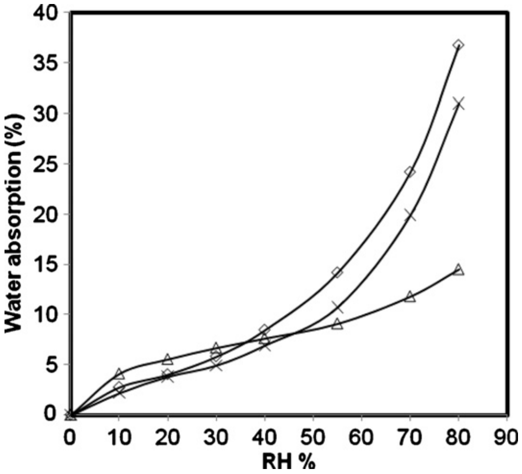

Fig. 5. Sorption isotherms for cellulose (△), starch + 19% glycerol (◊) and starch + 19% glycerol + 10% cellulose (×).

of the phase diagram, glycerol molecules show their intrinsic hydrophilicity.

The inflection point, where the evolution of the hydrophilicity is reversed for each relative humidity (10, 20, 30, 40 and 55 HR), corresponds to the intersection of the two trendlines obtained from (i) three or four points corresponding to the highest glycerol content (dotted line) and (ii) from the three or four points corresponding to the lowest glycerol content (solid curve).

The position of the inflection point is a function of relative humidity. At high RH, starch is mainly in interaction with water

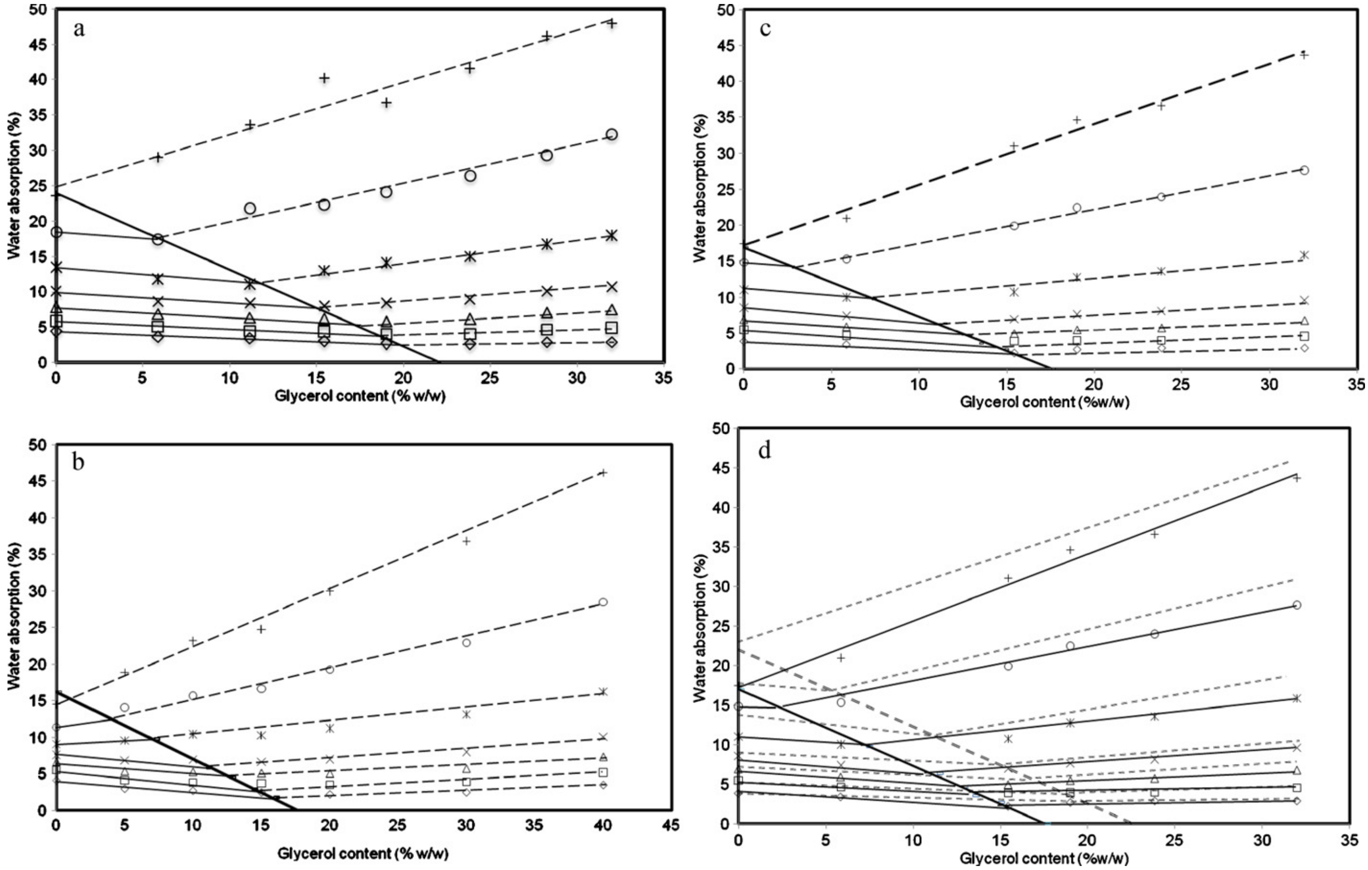

Fig. 6. Water sorption isotherms (water content) as a function of glycerol percentage at different ERH (10% (◊), 20% (□), 30% (△), 40% (×), 55% (*), 70% (◯), 80% (+)) of (a) starch, (b) cellulose, (c) TPS +10% cellulose, (d) TPS with 10% cellulose calculated "sim" (—) and experimental "exp" (—).

and a low quantity of glycerol leads to the saturation of sorption sites. At low RH, water is the minor interacting component.

A trendline of the inflections points was plotted ($R^2 = 0.9965$). Linear extrapolation of the inflection point to zero water content suggested a maximum quantity of 22% glycerol strongly sorbed onto starch. This quantity corresponds to a molar ratio of 0.5:1 glycerol for 2 anhydroglucose units. This does not correspond to the maximum interaction potential of these polyol molecules which both contain three hydroxyl groups. These results confirm the practical functionality of starch and glycerol noted earlier, i.e. one site on the anhydroglucose unit and two sites on glycerol. The main explanation for the low functionality of starch by glycerol is probably linked to sterical considerations.

As proposed for the determination of pure glycerol interaction with starch, the diagram in Fig. 6a can be extrapolated to zero glycerol content. The saturation concentration of starch by pure water is 24%. This corresponds to a stoichiometric ratio of 2.84 water molecules for 1 anhydroglucose unit, which can be approximated to a 3:1 ratio (this is roughly the case for 25% water content). Considering the functionality of anhydroglucose, this saturation condition could be described by the interaction of monofunctional water with a trifunctional anhydroglucose. This suggests that the anhydroglucose unit behaves as a trifunctional substrate towards water and as a monofunctional substrate towards glycerol. Consequentially, all intermediate ternary starch–glycerol–water compositions described by the “saturation straight line” correspond to a complex situation where water is in competition with glycerol for the interaction with high energy sites, but also where water is sorbed onto 2 other free sites.

This 3:1 stoichiometric ratio differs from the so-called BET monolayer where one water molecule interacts with two anhydroglucose unit (the first inflection of the sorption isotherm). On the contrary, this value is higher than the water saturation concentration deduced by Fringant et al. (1996) from sorption calorimetry measurements. In this study, the anhydroglucose unit was described by four sorption sites (three hydroxyl and one ketone function) in interaction with two bifunctional water molecules. Obviously, the stoichiometric ratio of the macromolecular substrate and the sorbed molecules depend on the property which is used for the definition of saturation phenomena. In our case, the criteria for polysaccharide saturation are defined from the beginning of a direct interaction of water with glycerol.

The behavior of cellulose–glycerol systems can be interpreted in the same way as the reference behavior of amorphous starch. The whole shape of the curve bundle obtained in Fig. 6b is close to the results in Fig. 6a. This suggests a common behavior of polysaccharides towards glycerol.

The extrapolation to zero water content leads to a maximum value of 17.5% glycerol in strong interaction with cellulose, versus 22% for a starch glycerol system. This can be attributed to the organization of the cellulose.

Fig. 6c shows the phase diagrams obtained for starch–glycerol–10% cellulose systems. As previously noted, the whole shape of the curve bundle is the same. In particular, the existence of a linear variation of the inflection point seems to be general. The extrapolation to zero water content can thus be considered as a characteristic value of binary and ternary systems.

The main difference between composite phase diagrams and that of plasticized starch is the position of the extrapolated point, which seems to be a decreasing function of cellulose content, i.e. 22% glycerol for 0% cellulose, 20% glycerol for 5% cellulose (data not shown), and 17.5% glycerol for 10% cellulose. In order to interpret these results, several diagrams, were calculated from the experimental behavior of the reference starch–glycerol system and the reference cellulose-glycerol system assuming no interactions (linear mixing laws). Different possibilities were calculated assuming different partitioning of glycerol between starch and cellulose: (i) glycerol totally distributed in the starch phase, (ii) glycerol distributed proportionally to the component content, (iii) glycerol uniformly distributed in starch and cellulose. Fig. 5e displays the example of the third assumption. For all the simulations, cellulose introduction does not drastically change the initial phase diagram of starch. Fig. 5e compares the calculated diagram to the experimental behavior of the composite. A clear difference in the position of the extrapolated point is observed. This cannot be attributed to the lower interaction potential of cellulose, taken into account by comparison to calculated data. The shift of the extrapolated point is also a result of the strong interactions between starch and cellulose, which decreases the capacity of the whole macromolecule blend to interact with glycerol.

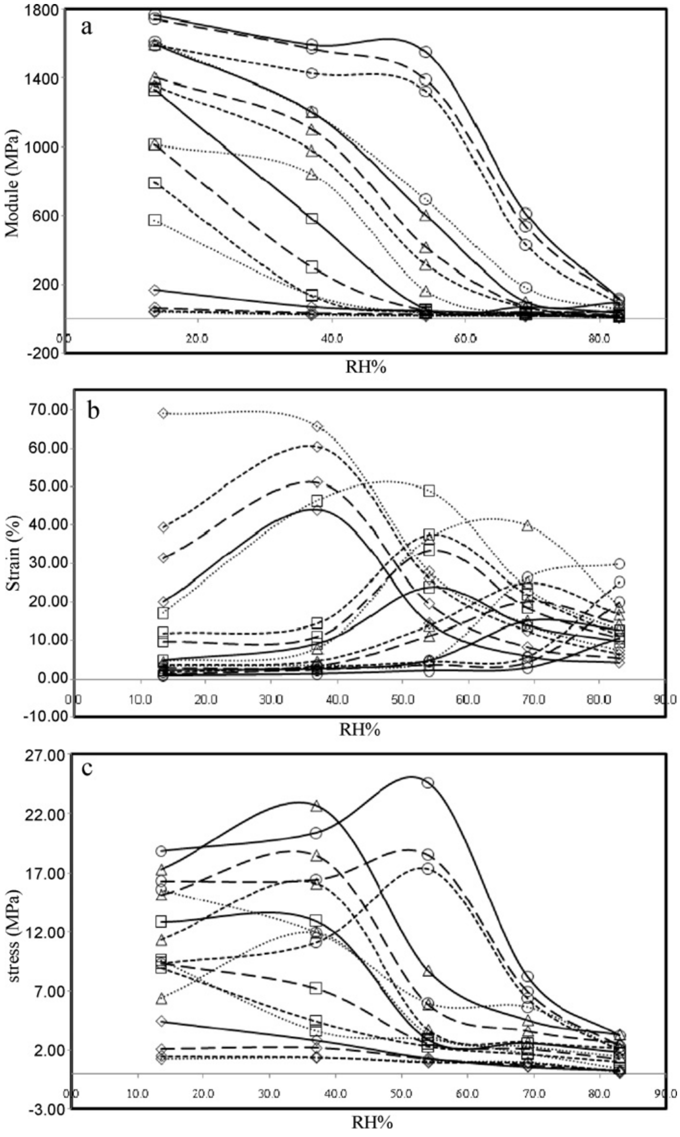

Fig. 7. The effect of water content on (a) the modulus, (b) strain and (c) stress of starch with the different glycerol content (6% (○), 15% (△), 24% (□), 32% (◇)) and different cellulose content (0% (···), 5% (–-), 10% (–––), 20% (—)).

In terms of interaction stoichiometry, the introduction of 0–5% and 5–10% cellulose decreases the glycerol maximum interaction from 22 to 20% and 20 to 17.5% respectively. In terms of molar ratio, the reduction of roughly 2% starch available for sorption with 5% cellulose would suggest a very high interaction of both polymers. As the systems interact only at interfaces, the consumption of starch sorption sites by cellulose could explain a *limited* decrease

Table 2
Average[a] and standard deviation[b] of stress (MPa), strain (%) and modulus (MPa).

	Strain (%)					Modulus (MPa)					Stress (MPa)				
RH (%)	13.5	37.0	54.0	69.0	83.0	13.5	37.0	54.0	69.0	83.0	13.5	37.0	54.0	69.0	83.0
S6G															
Av[a]	3.31	3.50	4.71	26.31	29.77	1612	1201	691	181	50	15.60	11.94	5.97	5.64	2.02
SD[b]	0.05	0.30	0.03	0.07	1.17	185	58	8	0.95	10	0.17	1.42	0.12	0.03	0.10
S6G5C															
Av	1.74	3.03	4.48	5.76	25.19	1589	1425	1321	429	81	9.32	11.08	17.35	6.40	1.99
SD	0.27	0.24	1.07	0.98	0.66	105	28.66	107	83	6	0.48	2.43	0.64	0.87	0.04
S6G10C															
Av	1.16	2.34	3.55	4.24	19.91	1742	1569	1389	535	107	16.32	16.45	18.54	6.95	2.34
SD	0.41	0.20	0.29	1.51	2.46	51	60.8	116.5	77.1	3.3	0.18	2.08	1.75	0.55	0.39
S6G20C															
Av	0.88	1.26	2.10	2.79	10.61	1764	1594	1551	611.7	116	18.84	20.39	24.61	8.21	3.23
SD	0.07	0.27	0.93	0.20	2.05	52.6	16.2	121.1	2.6	8.6	3.02	2.80	3.04	1.03	1.24
S15G															
Av	4.52	7.90	36.55	39.77	18.67	1013	842.1	160.8	23.5	18.2	6.38	11.88	3.32	2.27	1.45
SD	0.03	4.38	0.07	2.32	1.17	28.33	43.52	0.43	2.61	3.39	0.09	1.83	0.04	0.09	0.08
S15G5C															
Av	3.57	4.59	13.95	25.05	16.69	1353	978.3	315.38	64.88	37.8	11.31	16.12	3.74	2.69	2.16
SD	0.07	1.02	0.61	6.12	2.24	45.14	82.24	37.57	7.03	0.88	3.03	4.20	0.30	0.29	0.26
S15G10C															
Av	2.79	3.34	11.22	20.09	14.28	1402	1101	415	68.8	41.51	15.12	18.46	5.88	3.65	2.63
SD	0.47	0.61	2.85	2.13	0.79	110.7	219.2	89.5	8.1	4.02	2.86	3.90	0.99	0.16	0.49
S15G20C															
Av	2.33	2.66	4.87	15.22	12.86	1595	1201	602.3	98.01	93.66	17.31	22.71	8.71	4.54	3.31
SD	0.32	0.49	1.05	1.58	0.98	69.5	40.0	17.3	22.41	21.39	0.19	1.00	0.76	1.03	0.58
S24G															
Av	17.13	46.40	48.84	23.41	12.53	572	139	32.04	22.36	8.54	9.60	3.65	2.93	1.72	0.46
SD	0.53	0.28	0.13	0.67	0.92	2.2	1.65	0.48	3.54	0.12	0.08	0.02	0.04	0.34	0.09
S24G5C															
Av	12.03	14.54	37.53	21.98	11.32	789	132	37.53	26.37	16.48	8.95	4.46	2.34	1.69	1.04
SD	1.04	0.84	2.09	1.38	1.42	117.6	22.17	2.13	2.43	0.68	1.58	0.28	0.14	0.09	0.10
S24G10C															
Av	9.70	11.05	33.47	18.49	10.49	1013	300	45.75	37.21	20.44	9.36	7.22	2.55	2.10	1.23
SD	0.29	1.39	0.84	1.12	2.28	155.63	36.58	5.83	1.58	1.17	1.71	0.22	0.27	0.14	0.23
S24G20C															
Av	4.76	9.13	23.91	13.91	9.64	1331	582	54.15	65.92	31.04	12.83	12.91	2.86	2.58	1.80
SD	0.97	3.03	6.09	4.10	1.36	225.8	86.04	5.81	2.76	9.20	1.12	0.18	0.34	0.15	0.21
S32G															
Av	69.20	65.77	27.81	14.22	7.28	39.26	20.91	14.32	12.94	5.46	1.27	1.37	1.05	0.99	0.12
SD	9.60	0.14	0.44	2.39	1.68	2.84	0.03	1.58	0.65	1.11	0.01	0.03	0.02	0.20	0.11
S32G5C															
Av	39.32	60.36	25.95	12.45	6.33	41.91	24.04	18.05	15.57	6.62	1.51	1.43	0.97	0.91	0.18
SD	4.60	2.12	1.44	0.88	0.69	13.37	1.32	1.08	0.42	0.79	0.34	0.47	0.05	0.01	0.02
S32G10C															
Av	31.32	51.12	19.47	8.21	5.31	62.00	33.72	25.94	18.18	8.32	2.10	2.19	1.23	0.70	0.26
SD	9.99	2.43	1.12	1.09	0.96	24.24	2.38	1.58	2.22	0.88	0.53	0.34	0.14	0.13	0.05
S32G20C															
Av	20.04	44.02	14.49	5.83	4.16	166.38	67.52	43.95	26.95	12.44	4.44	2.83	1.31	0.57	0.29
SD	1.63	4.09	0.31	1.02	0.16	18.99	2.95	2.06	2.91	0.54	0.58	0.08	0.06	0.18	0.04

[a] Average.
[b] Standard deviation.

of the starch saturation point by glycerol, but not so large a variation of sorption behavior. Complex interactions probably involve the three components simultaneously. For example, structuration of starch on cellulose could decrease the availability of sorption site (transcristallinity-like phenomenon). This could explain the drastic shift of the extrapolated point (Yu et al., 2008) have shown a reduction to 15% glycerol for the position of the extrapolated point, using the same Godbillot et al. (2006) method. Their studied filler was sodium montmorillonite clay with a cation exchange capacity of 128 meq/100 g. The reduction of glycerol interaction with starch is also characteristic of a high interaction between filler and plasticized matrix. The simple direct use of data for stoichiometric interpretation of interactions still remains questionable.

The water content at the saturation point (extrapolation of “saturation straight line” to the *Y* axis) is reduced by the introduction of cellulose (from 24% to 17%). Once again, the effect of fiber introduction is drastic and cannot only be explained by consumption of sorption sites by starch/cellulose interactions. Complex interactions of the three components are probably involved.

3.3. *Mechanical properties*

Fig. 7 shows the mechanical properties of starch materials formulated with 0–32% glycerol and 0–20% cellulose. All of the systems were systematically characterized in different humidity environments, from 11 to 85% RH. Table 2 shows also the averages of five measurements and their standard deviation.

Some common observations can be made from Fig. 7a, showing the variation of the elastic modulus. A drastic decrease of the modulus was observed as a function of relative humidity, which can be associated to the glass transition. The higher the plasticizer content, the lower the position of the glass transition on the RH scale (Mali, Grossmann, García, Martino, & Zaritzky, 2004). The increase of cellulose content led to higher modulus values. Breaking properties (Fig. 7b) are obviously affected by the same plasticization (Mali, Sakanaka, Yamashita, & Grossmann, 2005) and reinforcing phenomena, with a “shift effect” of the glycerol content on the variation of breaking properties as a function of relative humidity. Negative and positive effects of cellulose content were respectively observed on strain at break and stress at break, as commonly seen in composites. The partition of glycerol between the starch matrix and fibers is also reported as a phenomenon that influences the Young modulus of composite films, due to the desplasticization of starch matrix (Kunanopparat, Menut, Morel, & Guilbert, 2008).

The strain at break shows a maximum value as a function of relative humidity. The same behavior was observed by Ma et al. (2005) and Talja, Helén, Roos, and Jouppila (2008) with filled thermoplastic starch. At low RH, this increase can be directly explained by a plasticization effect. At high RH the decrease of strain at break could be attributed to different phenomena such as the appearance of water and glycerol clusters, or material reorganization, which cannot be completely prevented due to the necessary time for material equilibration.

A similar variation was observed with the stress at break which presents a maximum value (Fig. 7c), but at much lower relative humidity than elongation at break.

The introduction of cellulose in the formulation leads to a drastic increase of the modulus and the stress at break, as observed by many authors working on biocomposites (Avérous et al., 2001; Martins et al., 2009; Müller et al., 2009). Generally, a continuous increase of the glass transition temperature is observed. In our study, the shift of the strain at break peak on the RH scale as a function of cellulose content was not continuous. An important shift was obtained after the introduction of 5% cellulose, but higher loading did not shift the position of the maximum peak any further. This would suggest that the “transition” defined by the maximum of strain at break (called after in the text “ultimate strain transition”) is not directly dependant on the glass transition.

4. Discussion

Fig. 8a shows the superposition of the phase diagram of unfilled plasticized starch, as defined by water sorption measurements, ultimate strain transition, and curves corresponding to different glass transition temperatures (17, 27 and 37 °C) obtained by Lourdin et al. This data can be considered as appropriate references for our work, as glass transition temperatures of amorphous glycerol plasticized starch have shown low variation as a function of starch natural origin.

The first observation is that the three transition lines are not located in the same place in the phase diagram. Moreover, the slopes of the straight lines are very dissimilar, suggesting a different dependence of the various properties of water when compared to glycerol.

The “saturation transition” and the “glass transition” can be considered as well defined phenomena. On the contrary, the “ultimate strain transition” probably depends on multiple factors. The straight line slope of the ultimate strain transition shows intermediate values compared to the low slope of the glass transition and the high slope of starch saturation, this suggests that the ultimate strain transition depends on a combination of polymer saturation and glass transition.

This interpretation is supported by previous work on plasticization/antiplasticization of starch (Lourdin, Bizot, & Colonna, 1997), which demonstrated that ultimate mechanical properties and barrier properties were controlled by a combination of beta transition increase and alpha transition decrease. Considering that the beta transition of starch is mainly affected by primary hydroxyl group interactions, our conclusions are very close to these previous studies. In the present paper, the starch/glycerol interaction stoichiometry was shown to be 1:0.5 (glucose to anhydroglucose). This suggests only one interaction site on starch towards glycerol which is probably the hydroxymethyl group (CH_2OH). This site has a stronger binding capacity compared to the other three binding sites on starch (Godbillot et al., 2006).

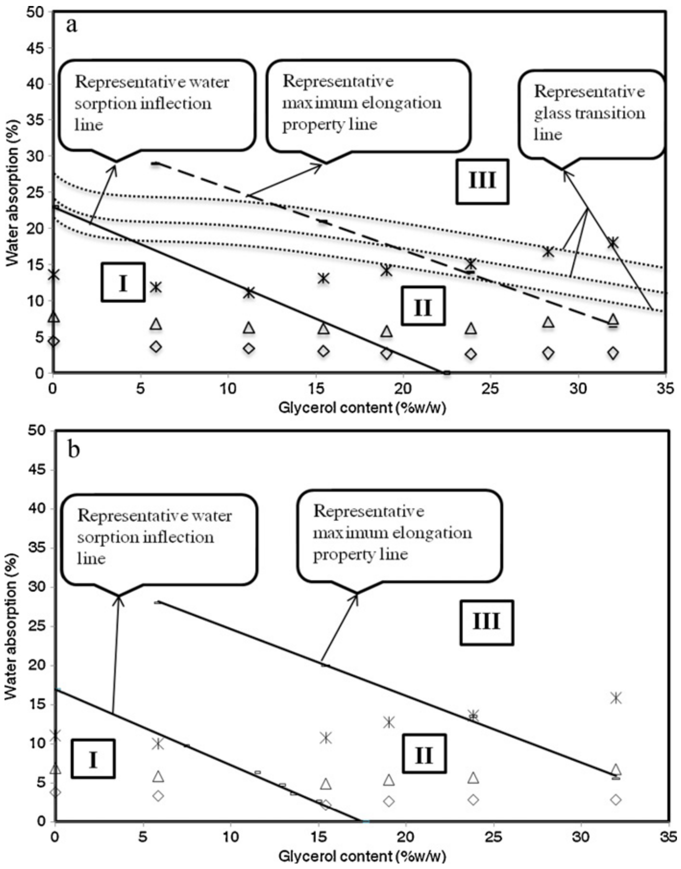

Fig. 8. (a) Water sorption isotherms (water content) as a function of glycerol percentage at different RH (10% (◊), 30% (△), 55% (*)) of starch with the location of three typical areas: (I) water and glycerol in strong interaction with starch, (II) water and glycerol in multilayers on starch and glycerol and (III) Presence of water and glycerol clusters. (b) Water sorption isotherms (water content) as a function of glycerol percentage at different RH (10% (◊), 30% (△), 55% (*)) of Starch +10% of cellulose with the location of three typical areas: (I) water and glycerol in strong interaction with starch and cellulose, (II) water and glycerol in multilayers on starch, glycerol and cellulose, (III) Presence of water and glycerol clusters.

Fig. 8b shows the evolution of Fig. 8a after cellulose introduction. Unfortunately, no glass transition (T_g) data can be superposed in this case, as literature data is probably not comparable because of the different types of cellulose T_g increases depend on the fiber length and must be due both to interfacial effects, strong H-bond interactions between polar components (e.g. carbohydrates), and to mechanical reinforcing effects (Averous & Boquillon, 2004). The position of the ultimate strain transition is shifted to higher glycerol content, while as discussed previously, the position of the saturation transition is shifted to lower glycerol content. In the absence of glass transition data it is not possible to confirm the dependence of ultimate strain transition on a combination of glass transition and saturation transition.

Another possible theory for the existence of the ultimate strain transition could be based on starch retrogradation, but all processes and characterization steps were defined in this work to guarantee amorphous systems. *Glycerol sursaturation* is a better explanation of the observed phenomena and is in good accordance with well known water–polysaccharides steps of interaction, i.e. bonded, multilayer and cluster forms of water. In the case of the “glycerol + water” system, the 3 states could be described as (i) the monolayer, which is quantified by the notion of interaction stoichiometry, as shown by the water sorption properties (ii) the multilayer at intermediate water activities and glycerol contents, and (iii) the cluster formation at high RH and glycerol content.

5. Conclusion

The existence of a well defined hard interaction between glycerol and starch was confirmed in this study. The saturation of starch is defined by a 2:1 anhydroglucose unit/glycerol stoichiometric ratio. In contrast to the functionality of starch towards water, not all the glucose hydroxyl units are involved in an interaction with glycerol. Only one group per anhydroglucose unit is involved with glycerol under the same criteria, saturation by water is obtained for a 1:3 anhydroglucose unit/water ratio.

Interpretating polymer plasticizer interaction in terms of stoichiometry constitutes an interesting field of research investigation, and opens a new approach in natural polymer plasticization. This supposes the attribution of functionality to plasticizers and polymers (Bouajila, Dole, Joly, & Limare, 2006); it also involves the calculation of concentrations in terms of molar ratios, while the science of polymer formulation is often approached in terms of mass or volume ratios.

The phase diagrams proposed in this paper can be useful for the interpretation of mechanical properties as a function of glycerol and water content. Further investigations are however necessary to better characterize complex systems such as highly hydrated and plasticized starch, and quaternary systems containing cellulose.

References

Amash, A., & Zugenmaier, P. (2000). Morphology and properties of isotropic and oriented samples of cellulose fibre-polypropylene composites. *Polymer*, *41*(4), 1589–1596.

Anglès, M. N., & Dufresne, A. (2001). Plasticized starch/tunicin whiskers nanocomposite materials. 2. Mechanical behavior. *Macromolecules*, *34*(9), 2921–2931.

Averous, L., & Boquillon, N. (2004). Biocomposites based on plasticized starch: Thermal and mechanical behaviours. *Carbohydrate Polymers*, *56*(2), 111–122.

Averous, L., & Fringant, C. (2001). Association between plasticized starch and polyesters: Processing and performances of injected biodegradable systems. *Polymer Engineering and Science*, *41*(5), 727–734.

Avérous, L., Fringant, C., & Moro, L. (2001). Plasticized starch–cellulose interactions in polysaccharide composites. *Polymer*, *42*(15), 6565–6572.

Averous, L., Moro, L., Dole, P., & Fringant, C. (2000). Properties of thermoplastic blends: Starch–polycaprolactone. *Polymer*, *41*(11), 4157–4167.

Baumberger, S., Lapierre, C., Monties, B., Lourdin, D., & Colonna, P. (1997). Preparation and properties of thermally moulded and cast lignosulfonates–starch blends. *Industrial Crops and Products*, *6*(3–4), 253–258.

Baumberger, S., Lapierre, C., Monties, B., & Valle, G. D. (1998). Use of kraft lignin as filler for starch films. *Polymer Degradation and Stability*, *59*(1–3), 273–277.

Bouajila, J., Dole, P., Joly, C., & Limare, A. (2006). Some laws of a lignin plasticization. *Journal of Applied Polymer Science*, *102*(2), 1445–1451.

Chang, Y., Cheah, P., & Seow, C. (2000). Plasticizing – Antiplasticizing effects of water on physical properties of tapioca starch films in the glassy state. *Journal of Food Science*, *65*(3), 445–451.

Chivrac, F., Pollet, E., Schmutz, M., & Avérous, L. (2008). New approach to elaborate exfoliated starch-based nanobiocomposites. *Biomacromolecules*, *9*(3), 896–900.

Cho, S. Y., & Rhee, C. (2002). Sorption characteristics of soy protein films and their relation to mechanical properties. *Lebensmittel-Wissenschaft und-Technologie*, *35*(2), 151–157.

Curvelo, A. A. S., de Carvalho, A. J. F., & Agnelli, J. A. M. (2001). Thermoplastic starch–cellulosic fibers composites: Preliminary results. *Carbohydrate Polymers*, *45*(2), 183–188.

de Carvalho, A. J. F., Curvelo, A. A. S., & Agnelli, J. A. M. (2001). A first insight on composites of thermoplastic starch and kaolin. *Carbohydrate Polymers*, *45*(2), 189–194.

Follain, N., Joly, C., Dole, P., & Bliard, C. (2005). Mechanical properties of starch-based materials. I. Short review and complementary experimental analysis. *Journal of Applied Polymer Science*, *97*(5), 1783–1794.

Forssell, P. M., Hulleman, S. H. D., Myllärinen, P. J., Moates, G. K., & Parker, R. (1999). Ageing of rubbery thermoplastic barley and oat starches. *Carbohydrate Polymers*, *39*(1), 43–51.

Fringant, C., Desbrières, J., Milas, M., Rinaudo, M., Joly, C., & Escoubes, M. (1996). Characterisation of sorbed water molecules on neutral and ionic polysaccharides. *International Journal of Biological Macromolecules*, *18*(4), 281–286.

Godbillot, L., Dole, P., Joly, C., Rogé, B., & Mathlouthi, M. (2006). Analysis of water binding in starch plasticized films. *Food Chemistry*, *96*(3), 380–386.

Helbert, W., Sugiyama, J., Ishihara, M., & Yamanaka, S. (1997). Characterization of native crystalline cellulose in the cell walls of oomycota. *Journal of Biotechnology*, *57*(1–3), 29–37.

Hulleman, S. H. D., Janssen, F. H. P., & Feil, H. (1998). The role of water during plasticization of native starches. *Polymer*, *39*(10), 2043–2048.

Ishikawa, A., Okano, T., & Sugiyama, J. (1997). Fine structure and tensile properties of ramie fibres in the crystalline form of cellulose I, II, IIII and IVI. *Polymer*, *38*(2), 463–468.

Kristo, E., & Biliaderis, C. G. (2006). Water sorption and thermo-mechanical properties of water/sorbitol-plasticized composite biopolymer films: Caseinate-pullulan bilayers and blends. *Food Hydrocolloids*, *20*(7), 1057–1071.

Kunanopparat, T., Menut, P., Morel, M. H., & Guilbert, S. (2008). Reinforcement of plasticized wheat gluten with natural fibers: From mechanical improvement to deplasticizing effect. *Composites Part A: Applied Science and Manufacturing*, *39*(5), 777–785.

Lourdin, D., Bizot, H., & Colonna, P. (1997a). "Antiplasticization" in starch–glycerol films? *Journal of Applied Polymer Science*, *63*(8), 1047–1053.

Lourdin, D., Bizot, H., & Colonna, P. (1997b). Correlation between static mechanical properties of starch–glycerol materials and low-temperature relaxation. *Macromolecular Symposia*, *114*, 179–185.

Lourdin, D., Coignard, L., Bizot, H., & Colonna, P. (1997). Influence of equilibrium relative humidity and plasticizer concentration on the water content and glass transition of starch materials. *Polymer*, *38*(21), 5401–5406.

Lourdin, D., Colonna, P., Brownsey, G. J., Noel, T. R., & Ring, S. G. (2002). Structural relaxation and physical ageing of starchy materials. *Carbohydrate Research*, *337*(9), 827–833.

Lourdin, D., Valle, G. D., & Colonna, P. (1995). Influence of amylose content on starch films and foams. *Carbohydrate Polymers*, *27*(4), 261–270.

Ma, X., Yu, J., & Kennedy, J. F. (2005). Studies on the properties of natural fibers-reinforced thermoplastic starch composites. *Carbohydrate Polymers*, *62*(1), 19–24.

Mali, S., Grossmann, M. V. E., García, M. A., Martino, M. N., & Zaritzky, N. E. (2004). Barrier, mechanical and optical properties of plasticized yam starch films. *Carbohydrate Polymers*, *56*(2), 129–135.

Mali, S., Sakanaka, L. S., Yamashita, F., & Grossmann, M. V. E. (2005). Water sorption and mechanical properties of cassava starch films and their relation to plasticizing effect. *Carbohydrate Polymers*, *60*(3), 283–289.

Martin, O., & Avérous, L. (2001). Poly(lactic acid): Plasticization and properties of biodegradable multiphase systems. *Polymer*, *42*(14), 6209–6219.

Martins, I. M. G., Magina, S. P., Oliveira, L., Freire, C. S. R., Silvestre, A. J. D., Neto, C. P., & Gandini, A. (2009). New biocomposites based on thermoplastic starch and bacterial cellulose. *Composites Science and Technology*, *69*(13), 2163–2168.

Monnet, D., Joly, C., Dole, P., & Bliard, C. (2010). Enhanced mechanical properties of partially beta-amylase trimmed starch for material applications. *Carbohydrate Polymers*, *80*(3), 747–752.

Müller, C. M. O., Laurindo, J. B., & Yamashita, F. (2009). Effect of cellulose fibers on the crystallinity and mechanical properties of starch-based films at different relative humidity values. *Carbohydrate Polymers*, *77*(2), 293–299.

Myllärinen, P., Partanen, R., Seppälä, J., & Forssell, P. (2002). Effect of glycerol on behaviour of amylose and amylopectin films. *Carbohydrate Polymers*, *50*(4), 355–361.

Onteniente, J. P., Etienne, F., Bureau, G., & Claude, J. (1996). Fully biodegradable lubricated thermoplastic starches: Water desorption on extruded samples. *Starch – Stärke*, *48*(1), 10–16.

Rindlav-Westling, A., Stading, M., Hermansson, A.-M., & Gatenholm, P. (1998). Structure, mechanical and barrier properties of amylose and amylopectin films. *Carbohydrate Polymers*, *36*(2–3), 217–224.

Shogren, R. L., & Jasberg, B. K. (1994). Aging properties of extruded high-amylose starch. *Journal of Polymers and the Environment*, *2*(2), 99–109.

Subramanian, K., Senthil Kumar, P., Jeyapal, P., & Venkatesh, N. (2005). Characterization of ligno-cellulosic seed fibre from wrightia tinctoria plant for textile applications – An exploratory investigation. *European Polymer Journal*, *41*(4), 853–861.

Talja, R. A., Helén, H., Roos, Y. H., & Jouppila, K. (2007). Effect of various polyols and polyol contents on physical and mechanical properties of potato starch-based films. *Carbohydrate Polymers*, *67*(3), 288–295.

Talja, R. A., Helén, H., Roos, Y. H., & Jouppila, K. (2008). Effect of type and content of binary polyol mixtures on physical and mechanical properties of starch-based edible films. *Carbohydrate Polymers*, *71*(2), 269–276.

Van Soest, J. J. G., & Borger, D. B. (1997). Structure and properties of compression-molded thermoplastic starch materials from normal and high-amylose maize starches. *Journal of Applied Polymer Science*, *64*(4), 631–644.

Yu, J. H., Wang, J. L., Wu, X., & Zhu, P. X. (2008). Effect of glycerol on water vapor sorption and mechanical properties of starch/clay composite films. *Starch – Stärke*, *60*(5), 257–262.

Zhao, R. X., Torley, P., & Halley, P. J. (2008). Emerging biodegradable materials: Starch- and protein-based bio-nanocomposites. *Journal of Materials Science*, *43*(9), 3058–3071.